



## Adsorption of Strontium from an Aqueous Solution by TiO<sub>2</sub>-Pillared Zeolite

Kris Tri Basuki<sup>1\*</sup>, Muni Fatuzzahroh<sup>1</sup>, Dhita Ariyanti<sup>1</sup>, Andri Saputra<sup>2</sup>

<sup>1</sup>Department of Nuclear Chemical Engineering, STTN-BATAN, Jl. Babarsari, Yogyakarta 55821, Indonesia

<sup>2</sup>Politeknik ATK Yogyakarta, Jl. Prof. Dr. Wirdjono Prodjodikoro, Bantul, Yogyakarta 55188, Indonesia

**Abstract.** Strontium is a heavy metal that is commonly found in many groundwater systems because of migration from historic nuclear waste storage sites. Its radiation effect can cause bone cancer, tumors, and leukemia. An economical and the most effective method to remove heavy metals from aqueous solutions is adsorption. In this study, we synthesized a TiO<sub>2</sub>-pillared zeolite to improve the adsorption efficiency of the zeolite. The TiO<sub>2</sub>-pillared zeolite was synthesized via the pillarization process. Adsorbent characterization was done using X-ray powder diffraction, which showed that TiO<sub>2</sub> was successfully pillared. Fourier-transform infrared spectroscopy showed a shift in the peak at a wavenumber of 3425.70 cm<sup>-1</sup>, which can be attributed to the addition of TiO<sub>2</sub>. A parameter study conducted using a batch experiment showed that optimal strontium adsorption took place at pH 5 and contact time of 80 min. The Freundlich adsorption isotherm fitted the experimental data well, illustrating the adsorption of strontium as being non-ideal, reversible, and multilayer adsorption that occurs on the heterogeneous surface of the TiO<sub>2</sub>-pillared zeolite. A thermodynamic study indicated that strontium adsorption on the TiO<sub>2</sub>-pillared zeolite was an endothermic process, takes place spontaneously, and is quite stable.

**Keywords:** Adsorption; Strontium; Titanium dioxide; Zeolite

### 1. Introduction

In Indonesia, nuclear technology usage has increased in the fields such as agriculture, advanced materials, food, nuclear medicine, and industrial manufacturing. However, this has resulted in an increase in radioactive waste. Toxicological and radiological effects caused by radioactive wastewater on human health and the ecosystem are serious concerns. Radioactive wastewaters commonly contain strontium, which is a pure beta emitter, has a half-life of 28.8 years, and is commonly found in groundwater systems near nuclear storage sites (Pathak, 2017). Strontium enters the human body through ingestion, and its radiation effects include bone cancer, tumors, and leukemia (Herhady et al., 2003). Because of its high radiological toxicity and relatively long half-life, strontium removal from aqueous solutions is of great interest.

Strontium removal has been attempted using membrane separation, ion exchange, chemical precipitation, and adsorption. For low-strength wastewaters, in particular, most of these processes are inefficient and expensive (especially ion exchange) (Hasan et al., 2019). In contrast, adsorption has been proven to be effective in reducing the concentration. Research on strontium adsorption has been carried out using several adsorbents, such

---

\*Corresponding author's email: [kristri\\_basuki@batan.go.id](mailto:kristri_basuki@batan.go.id), Tel.: +62-274-484085; Fax: +62-274-489715  
doi: [10.14716/ijtech.v12i3.4376](https://doi.org/10.14716/ijtech.v12i3.4376)

polyacrylonitrile(PAN)-zeolite (Yusan and Erenturk, 2011), Ca-alginate (Song et al., 2013), SBA-15 (Zhang et al., 2015), Chitosan-Fuller's earth beads (Hasan et al., 2019), and K<sub>2</sub>Ti<sub>4</sub>O<sub>9</sub> (Lee et al., 2018).

Adsorption using zeolites is a promising method. Their ion exchange capacity, selectivity (Taamneh and Sharadqah, 2016), chemical stability, low cost (Abdel-Rahman et al., 2011), and high adsorption capacity (Hong, et al., 2018, Sudibandriyo and Putri, 2020) allow zeolites to have a high adsorption performance. Research on strontium adsorption using PAN-zeolite composites has been conducted by Yusan and Erenturk (2011), but the adsorption capacity (strontium uptake) was very low (0.011 mg strontium / g adsorbent). Efforts to increase the zeolite's adsorption capacity were taken by pillaring the zeolite with certain compounds, such as TiO<sub>2</sub>. TiO<sub>2</sub> nanoparticles perform well as adsorbents as evidenced from previous studies for the absorption of tellurium (Zhang et al., 2010), chromium (VI) (Ren et al., 2017), and copper (II) (Thahir et al., 2018). This study aims to synthesize and characterize the TiO<sub>2</sub>-pillared zeolite and evaluate its adsorption capacity for strontium adsorption. The change in the interlayer distance or basal spacing in the TiO<sub>2</sub>-pillared zeolite was determined using X-ray powder diffraction (XRD). Fourier-transform infrared (FTIR) spectroscopy was used to determine the effect of adding TiO<sub>2</sub> on the bonds in the zeolite structure. A batch experiment was conducted to evaluate the adsorption capacity. Freundlich and Langmuir adsorption isotherms and thermodynamic studies were implemented to comprehensively understand the adsorption process.

## 2. Methods

Mordenite zeolite and distilled water were purchased from CV. Progo Mulyo, Yogyakarta, Indonesia. Chemicals used for the synthesis of the TiO<sub>2</sub>-pillared zeolite included sodium hydroxide, absolute ethanol, hydrogen chloride, and nitric acid, which were purchased from Merck, Darmstadt, Germany. Chemical used for adsorption was strontium nitrate, which was obtained from Merck, Darmstadt, Germany.

Instruments used for the characterization of the TiO<sub>2</sub>-pillared zeolite were the TM 3000 Hitachi scanning electron microscope (SEM), X-ray diffractometer by PANAnalytical Type X'pert PRO, and Thermo Scientific Nicolet iS10 FTIR spectrometer. The final concentrations of strontium were measured using the atomic absorption spectrometer, 2-Solar Series Thermo Electron Corp.

### 2.1. Zeolite Activation

The zeolite was crushed and sieved using a 300 mesh sieve. In a beaker, 100 g of zeolite was added to 200 mL of 1 M hydrogen chloride. At steady room temperature, the mixture was stirred for 3 h. The mixture was rinsed to neutral pH using distilled water. Then, it was dried at 250°C for 4 h in a drying oven. This procedure was followed according to that reported by Sani et al. (2009).

### 2.2. Synthesis of TiO<sub>2</sub>-Pillared Zeolite

To a 100 mL of absolute ethanol, 100 g of activated zeolite and 5 g of TiO<sub>2</sub> were added and continuously stirred for 5 h at steady room temperature. The formed photocatalyst was separated using the Whatman 41 filter. The mixture was then dried at 120°C for 5 h in a drying oven and calcined in a furnace at 500°C for 5 h. Then, the obtained TiO<sub>2</sub>-pillared zeolite was characterized using SEM, XRD, and FTIR spectroscopy. According to Nikazar et al. (2007), the proposed incorporation of TiO<sub>2</sub> into the zeolite is as shown in Figure 1.

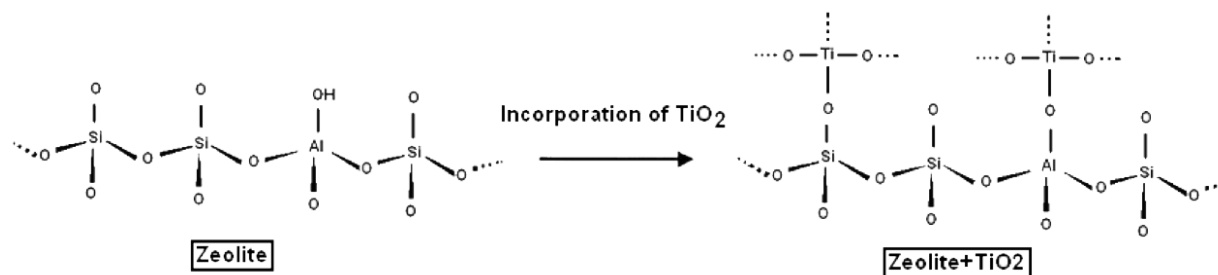


**Figure 1** Proposed incorporation of TiO<sub>2</sub> on the zeolite (Nikazar et al., 2007)

### 2.3. Batch Experiment to Analyze Strontium Adsorption

The effects of the adsorption parameters were analyzed via a batch experiment in triplo. A stock solution of 100 ppm of strontium was prepared by dissolving 0.241 g of strontium nitrate in 1 L of distilled water. 10 mL of strontium stock solution (at pH 5) was tested with 0.1 g of the TiO<sub>2</sub>-pillared zeolite at 25°C for different contact times (20, 40, 60, 80, and 100 min). The steps were repeated at different pH (4, 5, 6, 7, and 8) and various strontium concentrations (20, 40, 60, 80, 100, 120, 140, and 160 ppm). Atomic absorption spectroscopy (AAS) at a wavelength of 460.7 nm was used to measure the final concentrations of strontium (Qiu et al., 2018).

Adsorption isotherms were obtained and thermodynamic studies were conducted for the adsorption observed in the batch experiment conducted in triplo. 10 mL of strontium stock solution (optimal pH was found to be 5) was tested with 0.1 g of the TiO<sub>2</sub>-pillared zeolite 25°C for 100 min. This was repeated at various strontium concentrations (20, 40, 60, 80, and 100 ppm) and temperatures (25, 30, and 33°C). AAS at a wavelength of 460.7 nm was used to measure the final concentrations of strontium (Qiu et al., 2018).

## 3. Results and Discussion

### 3.1. Characterization of the TiO<sub>2</sub>-Pillared Zeolite

The TiO<sub>2</sub>-pillared zeolite was characterized by SEM, XRD, and FTIR spectroscopy. The zeolite FTIR spectra are illustrated in Figure 2. Figure 2a shows that O–H stretching vibrations correspond to the wavelength of 3413.12 cm<sup>-1</sup>. The adsorption at wavenumber 1647.26 cm<sup>-1</sup> indicates the functional groups of OH and the adsorption at wavenumbers 1047.38 cm<sup>-1</sup> and 796.63 cm<sup>-1</sup> indicate the presence of functional groups in the form of O–Si–O and O–Al–O. The uptake at wavenumber 453.29 cm<sup>-1</sup> is a characteristic of Al–O bonds. Whereas the FTIR spectra for the TiO<sub>2</sub>-pillared zeolite in Figure 2b shows a shift in the uptake at wavenumber 3452.70 cm<sup>-1</sup>, which corresponds to the O–H bond adsorption. The uptake at wavenumber 1643.41 cm<sup>-1</sup> refers to the functional groups of buckling OH. These FTIR spectroscopy results suggest a very small shift in the spectra between the zeolite and the TiO<sub>2</sub>-pillared zeolite, which is because they are still in the same range. The shift was caused by the addition of TiO<sub>2</sub> as well as the presence of other metals as contaminants in the zeolite such as silicon, aluminum, magnesium, sodium, potassium, calcium, and iron.

Figure 3a shows the SEM images of the zeolite morphology before being pillarized with TiO<sub>2</sub>. It is clear that there are several impurities mentioned above, making the distribution of TiO<sub>2</sub> not clearly visible. In Figure 3b, clear spots representing TiO<sub>2</sub> attached to the surface of the zeolite structures are visible. Thus, the SEM analysis clarifies that TiO<sub>2</sub> has been successfully pillarized on the zeolite.

The XRD data in Figure 4a show the zeolite diffraction spectra with diffraction angle 2θ at 13.50°, 19.53°, 25.52°, and 27.52°; this is a characteristic of mordenite minerals (M). A characteristic of the clinoptilolite (KI) mineral is found at 9.76° and 22.14°. Quartz minerals

give reflection with intensity in the region of  $2\theta$  at  $26.42^\circ$ . Therefore, the zeolite used in this study contains mordenite and clinoptilolite.

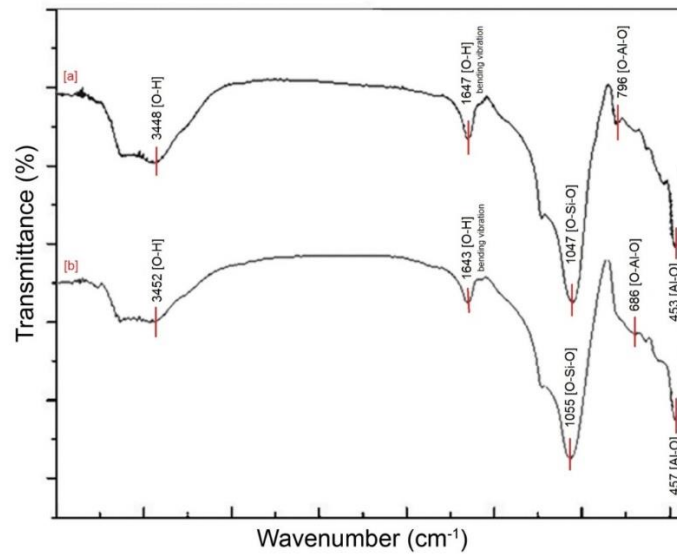


**Figure 2** Fourier-transform infrared spectra of the: (a) zeolite; and (b) TiO<sub>2</sub>-pillared zeolite

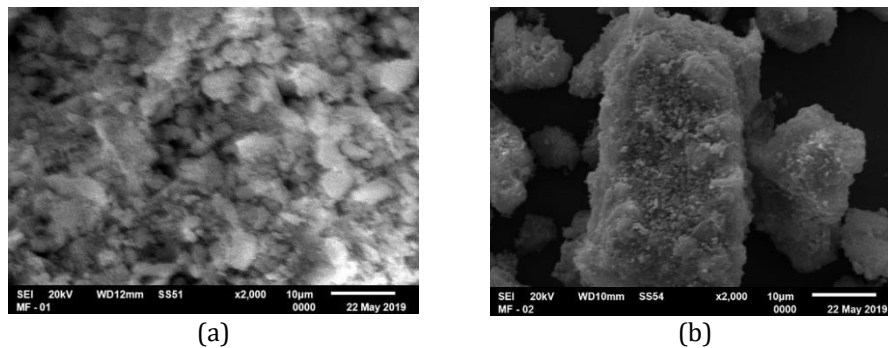


**Figure 3** Scanning electron microscopy images of the: (a) zeolite; and (b) TiO<sub>2</sub>-pillared zeolite

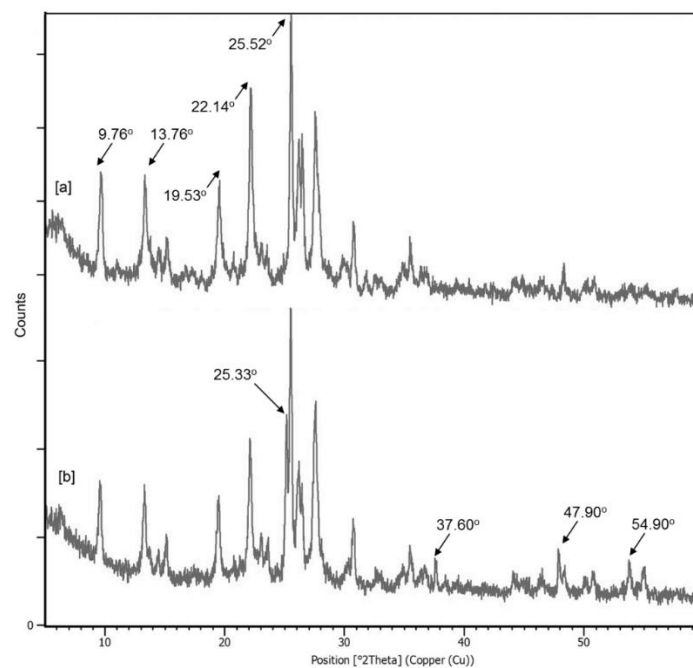


**Figure 4** X-ray powder diffraction spectra of the: (a) zeolite; and (b) TiO<sub>2</sub>-pillared zeolite

The TiO<sub>2</sub>-pillared zeolite diffraction spectra illustrated in Figure 4b has diffraction angle  $2\theta$  at 25.33°, 37.6°, 47.9°, and 54.9°, which are characteristic peaks of TiO<sub>2</sub>. TiO<sub>2</sub> anatase has been used in this study. The crystal structure difference between the anatase and rutile types lies in the distortion and arrangement of the octahedron chain (Pataya et al., 2016). The bond distance of Ti–Ti in anatase is higher than that in rutile. However, the bond distance of Ti–O in anatase is lower than that in rutile. Thus, TiO<sub>2</sub> anatase has a greater surface area than rutile. In the TiO<sub>2</sub>-pillared zeolite diffraction spectra, the characteristic peaks of TiO<sub>2</sub> reappeared, confirming that TiO<sub>2</sub> was immobilized on the surface of the zeolite.

### 3.2. Adsorption Study

#### 3.2.1. Effect of contact time

As illustrated in Figure 5a, as the contact time increased, the adsorption capacity ( $q_t$ ) increased. The adsorption of strontium reached equilibrium in 80 min. It is presumed that the diffusion of strontium from the bulk solution to the TiO<sub>2</sub>-pillared zeolite surface is controlled by the affinity of strontium toward the active binding sites of the zeolite, justifying the longer time needed for the adsorption to reach equilibrium. The adsorption capacity decreased after 80 min, which is caused by the TiO<sub>2</sub>-pillared zeolite releasing bonds with the adsorbate (i.e., desorption).

#### 3.2.2. Effect of initial concentration

To study the effect of initial strontium concentration, experiments were carried out using 10 mL of strontium stock solution (at pH 5), which was tested with 0.1 g of TiO<sub>2</sub>-pillared zeolite at 298 K for 80 min. Figure 5b illustrates that an increase in the initial concentration of strontium increases the adsorption capacity ( $q_t$ ). This is in line with the results of Zhao and Asuha (2010) and Ren et al. (2017). As the concentration of strontium increases, the driving force increases to overcome the mass transfer resistance of strontium from the aqueous solution into TiO<sub>2</sub>-Pillared Zeolite, which increases the adsorption equilibrium of the TiO<sub>2</sub>-pillared zeolite until it reaches a saturated state. Figure 5b also shows that the active sites of the TiO<sub>2</sub>-pillared zeolite are saturated with strontium when the initial concentration of strontium is 100 ppm.

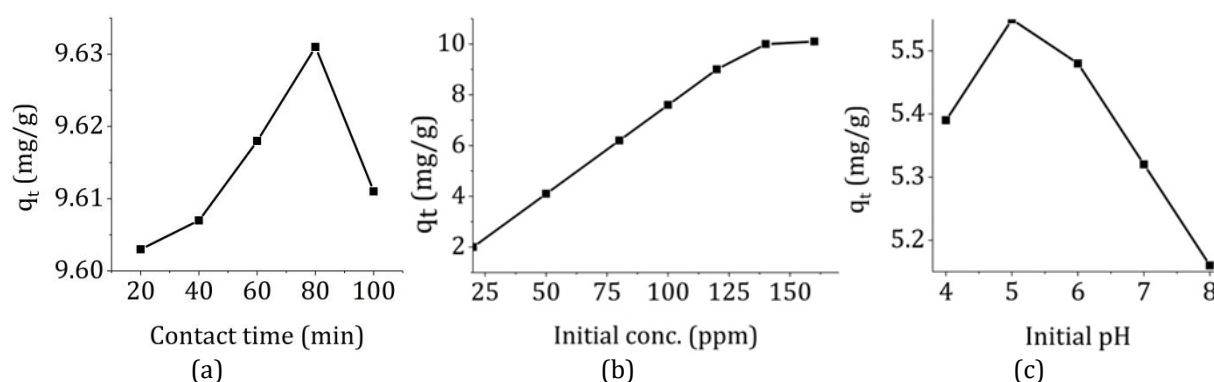


**Figure 5** Effect of: (a) contact time; (b) initial strontium concentration; and (c) initial pH of the aqueous solution on the strontium adsorption by the TiO<sub>2</sub>-pillared zeolite

#### 3.2.3. Effect of initial pH of the solution

According to Nishiyama et al. (2015), strontium adsorption increases with an increase in pH. To study the effect of initial pH, experiments were conducted using 10 mL of strontium stock solution with 100 ppm of strontium at pH ranging from 4 to 8. This was tested with 0.1 g of TiO<sub>2</sub>-pillared zeolite at 298 K for 80 min. It is evident that the adsorption capacity increases as the pH increases from 4 to 5. Lower adsorption capacity values at

lower pH is due to the competition of H<sup>+</sup> ions with strontium ions on the surface of the TiO<sub>2</sub>-pillared zeolite. In other words, at lower pH, the high ionic strength of H<sup>+</sup> and other cations compete with strontium to bind with the zeolite, thereby decreasing the adsorption capacity (Alswata et al., 2017).

### 3.3. Adsorption Isotherms

The performance of the TiO<sub>2</sub>-pillared zeolite was studied for strontium adsorption by using Langmuir (Equation 1) and Freundlich (Equation 2) (Desmiarti et al., 2019) adsorption isotherms. The interaction between strontium and the zeolite, homogeneity of the zeolite, and type of adsorption coverage can be described by these isotherm models (Kyzas et al., 2014).

$$\frac{C_e}{q_e} = \frac{1}{q_m K_L} + \frac{1}{q_m} C_e, \quad (1)$$

$$\ln(q_e) = \ln(K_F) + \frac{1}{n} \ln(C_e), \quad (2)$$

where  $C_e$  (mg/L) is the equilibrium concentration,  $q_e$  (mg/g) is equilibrium adsorption capacity,  $q_m$  is the adsorption capacity of a complete monolayer (mg/g),  $K_F$  is the Freundlich constant (mg/g)(L/mg)<sup>n</sup>,  $K_L$  is Langmuir constant (L/mg), and  $1/n$  is adsorption intensity or the heterogeneity factor, which ranges from 0 to 1 and is a characteristic of surface heterogeneity, indicating higher homogeneity when the value is closer to unity (Dada et al., 2012).

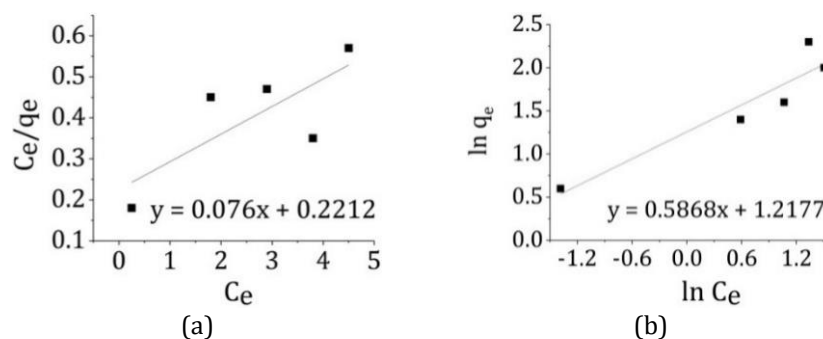
As illustrated in Figure 6, the obtained experimental data were fitted well with the Freundlich model than with the Langmuir model, which illustrates that the adsorption of strontium is defined as adsorption on a heterogeneous surface and as being non-ideal, reversible, and multilayer adsorption onto the heterogeneous surface of TiO<sub>2</sub>-pillared zeolite. Thus, the monolayer adsorption of strontium is not effective. Previous research by Seidlerová et al., (2016) has shown that TiO<sub>2</sub>-based adsorbents have a heterogeneous surface, which is in line with our result. Further, the zeolite-based adsorbents researched by Taamneh and Sharadqah (2016) fitted well with the Freundlich model. The  $1/n$  value for our Freundlich model, shown in Table 2, is 0.5868, which implies more heterogeneity as it is closer to unity. In this study, the strontium uptake is about 9.632 mg/g, which is lower than that compared with other studies using adsorbents such as SBA-15, Chitosan-Fuller's earth beads, modified bentonite, modified gibbsite, and K<sub>2</sub>Ti<sub>4</sub>O<sub>9</sub>, but it is superior to the uptake by PAN-zeolite and Ca-alginate. However, the time for the TiO<sub>2</sub>-pillared zeolite to reach equilibrium is shorter than that taken by the other adsorbents (see Table 1). This is the advantage of the TiO<sub>2</sub>-pillared zeolite over the other adsorbents.

**Table 1** Strontium uptake using various adsorbents

Adsorbent	Initial Concentration (mg/L)	Contact Time (h)	pH	Uptake (mg/g)	Reference
PAN-zeolite	25–175	0.33	5	0.011	Yusan and Erenturk (2011)
Ca-alginate	10–500	8	7	6.700	Song et al. (2013)
SBA-15	0–80	5	6	17.670	Zhang, et al. (2015)
Chitosan-Fuller's earth beads	20–1000	24	6.5	30.580	Hasan et al. (2019)
K <sub>2</sub> Ti <sub>4</sub> O <sub>9</sub>	5–200	12	7–7.5	70.900	Lee at al. (2018)
TiO <sub>2</sub> -pillared zeolite	25–150	1.3	5	9.632	Present work

**Table 2** Isotherm parameters

	Langmuir model	Freundlich model		Freundlich model
$q_m$	13.1547	$1/n$	0.5868	
$K_L$	0.3436	$K_F$	3.3794	
$R^2$	0.6400	$R^2$	0.9121	

**Figure 6** (a) Langmuir and (b) Freundlich adsorption isotherm models for strontium adsorption by the TiO<sub>2</sub>-pillared zeolite

### 3.4. Adsorption Thermodynamics

The experimental data were fitted into the linearized Equation (3) to obtain the thermodynamic parameters, namely entropy ( $\Delta S_{ads}^{\circ}$ ) and enthalpy ( $\Delta H_{ads}^{\circ}$ ) (Kumar et al., 2010), and the result is illustrated in Figure 7. The  $\Delta H_{ads}^{\circ}$  and  $\Delta S_{ads}^{\circ}$  values were obtained from the slope and intercept of the straight line in the graph, respectively, and the results have been tabulated in Table 2. The positive value of  $\Delta H_{ads}^{\circ}$  implies that the adsorption is endothermic (Fathy et al., 2016), indicating that the adsorption is not suitable to be conducted at low temperatures. The lower the  $\Delta S_{ads}^{\circ}$  value, the more stable is the process of running the reaction (Prihatiningsih et al., 2020). The obtained  $\Delta S_{ads}^{\circ}$  value is 0.0860, which indicates that the adsorption is quite stable.

$$\log \left( \frac{C_{Ae}}{C_e} \right) = - \frac{\Delta H_{ads}^{\circ}}{2.303 R T} + \frac{\Delta S_{ads}^{\circ}}{2.303 R} \quad (3)$$

The thermodynamic Gibbs free energy ( $\Delta G_{ads}^{\circ}$ ) was evaluated using Equation 4 at different temperatures (298, 303, and 313 K), where  $R$  is the gas constant (8.314 J/mol.K), and  $T$  is the temperature in Kelvin (K) (Hannachi et al., 2014).

$$\Delta G_{ads}^{\circ} = \Delta H_{ads}^{\circ} - T(\Delta S_{ads}^{\circ}) \quad (4)$$

The  $\Delta G_{ads}^{\circ}$  data in Table 3 show that an increase in temperature decreases the  $\Delta G_{ads}^{\circ}$ , suggesting that higher temperature is favorable for adsorption (Bhaumik et al., 2012). The negative value of  $\Delta G_{ads}^{\circ}$  indicates that the adsorption takes place spontaneously (Kutahyali and Eral, 2004), and the higher the negative value, the more energetically favorable the adsorption is. This is in line with the results of Yusan and Erenturk (2011). They show that strontium adsorption by PAN-zeolite takes place spontaneously.

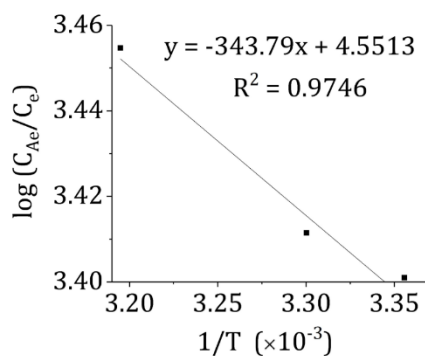


**Figure 7** Thermodynamic study on strontium adsorption by the TiO<sub>2</sub>-pillared zeolite

**Table 3** Thermodynamic parameters

Temperature (K)	Thermodynamic parameters			
	$C_{Ae}/C_e$	$\Delta G^\circ$ (kJ/mol)	$\Delta H^\circ$ (kJ/mol.K)	$\Delta S^\circ$ (kJ/mol)
298	2518	-19.3864		
303	2579	-19.8222	6.5826	0.0871
313	2849	-20.6936		

#### 4. Conclusions

The zeolite was successfully pillared by TiO<sub>2</sub>. Diffraction angle  $2\theta$  peaks of TiO<sub>2</sub> were found at 25.33°, 36.7°, 47.9°, and 54.9°. The FTIR spectra showed that the shift at wavenumber 3425.70 cm<sup>-1</sup> occurs due to the addition of TiO<sub>2</sub>. Based on the batch experiment results, the best parameters for strontium adsorption were found to be pH 5 and contact time of 80 min. The adsorption of strontium by the TiO<sub>2</sub>-pillared zeolite is defined as adsorption on a heterogeneous surface and as being non-ideal, reversible, and multilayer adsorption. Although the adsorption capacity is low, the thermodynamic study indicated that the adsorption of strontium onto TiO<sub>2</sub> pillared zeolite was an endothermic process that takes place spontaneously and is quite stable. For future work, the adsorption capacity needs to be increased, which can be accomplished by reducing the size of the pillared TiO<sub>2</sub> to allow more area for strontium to be absorbed.

#### References

- Abdel-Rahman, R.O., Ibrahim, H.A., Yung-Tse, H., 2011. Liquid Radioactive Wastes Treatment: A Review. *Water*, Volume 3(2), pp. 551–565
- Alswata, A.A., Ahmad, M.B., Al-Hada, N.M., Kamari, H.M., Hussein, M.Z.B., Ibrahim, N.A., 2017. Preparation of Zeolite/Zinc Oxide Nanocomposites for Toxic Metals Removal from Water. *Results in Physics*, Volume 7, pp. 723–731
- Bhaumik, R., Mondal, M.K., Das, B., Roy, P., Pal, K.C., Das, C., Banerjee, A., Datta, J.K., 2012. Eggshell Powder as an Adsorbent for Removal of Fluoride from Aqueous Solution: Equilibrium, Kinetic and Thermodynamic Studies. *European Journal of Advanced Chemistry Research*, Volume 9(3), pp. 1457–1480
- Dada, A.O., Olalekan, A.P., Olatunya, A.M., Dada, O., 2012. Langmuir, Freundlich, Temkin and Dubinin–Radushkevich Isotherms Studies of Equilibrium Sorption of Zn<sup>2+</sup> Onto Phosphoric Acid Modified Rice Husk. *IOSR Journal of Applied Chemistry*, Volume 3(1), pp. 38–45



- Desmiarti, R., Trianda, Y., Martynis, M., Viqri, A., Yamada, T., Li, F., 2019. Phenol Adsorption in Water by Granular Activated Carbon from Coconut Shell. *International Journal of Technology*, Volume 10(8), pp. 1488–1497
- Fathy, M., Moghny, T.A., Mousa, M.A., El-Bellihi, A.H.A.A, Awadallah, A.E., 2016. Absorption of Calcium Ions on Oxidized Graphene Sheets and Study its Dynamic Behavior by Kinetic and Isothermal Models. *Applied Nanoscience*, Volume 6(8), pp. 1105–1117
- Hasan, S., Iasir, A.R.M., Ghosh, T.K., Gupta, B.S., Prelas, M.A., 2019. Characterization And Adsorption Behavior of Strontium from Aqueous Solutions onto Chitosan-Fuller's Earth Beads. *Healthcare*, Volume 7(1), pp. 1–18
- Hannachi, C., Guesmi, F., Missaoui, K., Hamrouni, B., 2014. Application of Adsorption Models for Fluoride, Nitrate, and Sulfate Ion Removal by Amx Membrane. *International Journal of Technology*, Volume 5(1), pp. 60–69
- Herhady, R.D., Kusnanto, G., Sukarsono, R., Masduki, B., 2003. Sintesis Gelas Keramik Lithium Alumina Silikat untuk Imobilisasi Simulasi Limbah Stronsium-90 (*Synthesis of Lithium Alumina Silicate Ceramic Glass for Simulated Immobilization of Strontium-90 Waste*). *Indonesian Journal of Science and Technology*, Volume 4(4), pp. 107–119
- Hong, M., Yu, L., Wang, Y., Zhang, J., Chen, Z., Dong, L., Zan, Q., Ruili, L., 2018. Heavy Metal Adsorption with Zeolites: The Role of Hierarchical Pore Architecture. *Chemical Engineering Journal*, Volume 359, pp. 363–372
- Kumar, P.S., Ramakrishnan, K., Kirupha, S.D., Sivanesan, S., 2010. Thermodynamic and Kinetic Studies of Cadmium Adsorption from Aqueous Solution onto Rice Husk. *Brazilian Journal of Chemical Engineering*, Volume 27(02), pp. 347–355
- Kutahyali, C., Eral, M., 2004. Selective Adsorption of Uranium from Aqueous Solutions using Activated Carbon Prepared from Charcoal by Chemical Activation. *Separation and Purification Technology*, Volume 40(2), pp. 109–114
- Kyzas, G.Z., Deliyanni, E.A., Matis, K.A., 2014. Graphene Oxide and its Application as an Adsorbent for Wastewater Treatment. *Journal of Chemical Technology and Biotechnology*, Volume 89(2), pp. 196–205
- Lee, T., Na, C.K., Park, H., 2018. Adsorption Characteristics of Strontium onto  $K_2Ti_4O_9$  and PP-G-AA Nonwoven Fabric. *Environmental Engineering Research*, Volume 23(3), pp. 330–338
- Nikazar, M., Gholivand, K., Mahanpoor, K., 2007. Enhancement of Photocatalytic Efficiency of  $TiO_2$  by Supporting on Clinoptilolite in the Decolorization of Azo Dye Direct Yellow 12 Aqueous Solutions. *Journal of the Chinese Chemical Society*, Volume 54(5), pp. 1261–1268
- Nishiyama, Y., Hanafusa, T., Yamashita, J., Yamamoto, Y., Ono, T., 2015. Adsorption and Removal of Strontium in Aqueous Solution by Synthetic Hydroxyapatite. *Journal Of Radioanalytical and Nuclear Chemistry*, Volume 307, pp. 1279–1285
- Qiu, L., Feng, J., Dai, Y., Chang, S., 2018. Mechanisms of Strontium's Adsorption by *Saccharomyces Cerevisiae*: Contribution of Surface and Intracellular Uptakes. *Chemosphere*, Volume 215, pp. 15–24
- Pataya, S.A., Gareso, P.L., Juarlin, E., 2016. Karakterisasi Lapisan Tipis Titanium Dioksida ( $TiO_2$ ) yang Ditumbuhkan dengan Metode Spin Coating Diatas Substrat Kaca (*Characterization of a Layer of Titanium Dioxide ( $TiO_2$ ) that is Grown using Spin Coating Method on a Glass Substrate*). *Jurnal kimia*, pp. 1–8
- Pathak, P., 2017. An Assessment of Strontium Sorption onto Bentonite Buffer Material in Waste Repository. *Environmental Science and Pollution Research*, Volume 24(9), pp. 8825–8836

- Prihatiningsih, M.C., Basuki, K.T., Brawijaya, P., Saputra, A., 2020. The Adsorption Isotherm and Thermodynamic Studies of Rhenium onto Mesoporous Silica Nanoparticles. *Journal of Physics: Conference Series*, Volume 1436, pp. 1–8
- Ren, G., Wang, X., Huang, P., Zhong, B., Zhang, Z., Yang, L., Yang, X., 2017. Chromium (VI) Adsorption from Wastewater using Porous Magnetite Nanoparticles Prepared from Titanium Residue by a Novel Solid-Phase Reduction Method. *Science of the Total Environment*, Volume 607–608, pp. 900–910
- Sani, A., Rosita, A., Rakhmawaty, D., 2009. Pembuatan Fotokatalis TiO<sub>2</sub>-Zeolit Alam Asal Tasikmalaya untuk Fotodegradasi Methylene Blue (*Preparation of Natural Tio<sub>2</sub>-Zeolite Photocatalyst from Tasikmalaya for the Photodegradation of Methylene Blue*). *Jurnal Zeolit Indonesia*, Volume 8(1), pp. 6–14
- Seidlerová, J., Šafařík, I., Rozumová, L., Šafaříková, M., Motyka, O., 2016. TiO<sub>2</sub>-based Sorbent of Lead Ions. *Procedia Materials Science*, Volume 12, pp. 147–152
- Song, D., Park, S.J., Kang, H.W., Park, S.B., Han, J.I., 2013. Recovery of Lithium (I), Strontium (II) and Lanthanum (III) using Ca-alginate Beads. *Journal of Chemical & Engineering Data*, Volume 58(9), pp. 2455–2464
- Sudibandriyo, M., Putri, F.A., 2020. The Effect of Various Zeolites as an Adsorbent for Bioethanol Purification using a Fixed Bed Adsorption Column. *International Journal of Technology*, Volume 11(7), pp. 1300–1308
- Taamneh, Y., Sharadqah, S., 2016. The Removal of Heavy Metals from Aqueous Solution using Natural Jordanian Zeolite. *Applied Water Science*, Volume 7, pp. 2021–2028
- Thahir, R., Rosalin., Khaerunnisa., Laurenz, S., Puspitasari., 2018. Preparasi dan Karakterisasi Titanium Dioksida (TiO<sub>2</sub>) Mesopori Sebagai Adsorben Logam Cu(II) dan Methylene Blue (*Preparation and Characterization Of Mesoporous Titanium Dioxide (TiO<sub>2</sub>) as Adsorbent for Cu (II) and Methylene Blue*). In: Seminar Nasional Hasil Penelitian & Pengabdian Kepada Masyarakat (SNP2M) 2018 Dec 30, pp. 53–57
- Yusan, S., Erenturk, S., 2011. Adsorption Characterization of Strontium on PAN/Zeolite Composite Adsorbent. *World Journal of Nuclear Science and Technology*, Volume 1(01), pp. 6–12
- Zhang, L., Zhang, M., Liu, X., Kang, P., Chen, X., 2010. Sorption Characteristics and Separation of Tellurium Ions from Aqueous Solutions using Nano-TiO<sub>2</sub>. *Talanta*, Volume 83(2), pp. 344–350
- Zhang, N., Liu, S., Jiang, L., Luo, M., Chi, C., Ma, J., 2015. Adsorption of Strontium from Aqueous Solution by Silica Mesoporous SBA-15. *Journal of Radioanalytical and Nuclear Chemistry*, Volume 303, pp. 1671–1677
- Zhao, S., Asuha, S., 2010. One-pot Synthesis of Magnetite Nanopowder and their Magnetic Properties. *Powder Technology*, Volume 197(3), pp. 295–297